Short-Period Nonseismic Tilt Perturbations and Their Relation to Episodic Slip on the San Andreas Fault in Central California

STUART MCHUGH AND M. J. S. JOHNSTON

U.S. Geological Survey, Menlo Park, California 94025

Data from four tilt meters and several creep meters along the San Andreas fault in central California 30 km south of Hollister were selected to investigate nonseismic short-period tilt perturbations of minutes to hours duration. The group of short-period tilt amplitude changes with residual deflections was chosen because many nonseismic creep events have similar durations. Although each of the four tilt meters recorded many short-period events, the distribution in space and time suggests that most of these events are due to causes other than slip on the San Andreas fault, such as local strain release. Only at one station used in this investigation (MEL) were creep-related tilt changes observed. A quasi-static dislocation model was constructed to predict the tilt changes associated with propagating slip. Comparing predicted to observed tilt wave forms and amplitudes and comparing the tilt event data to creep event data suggest that (1) a tilt amplitude change of 10^{-8}–10^{-6} rad associated with nonseismic creep events will be observed only if the tilt meter is less than 0.5–1.0 km from the fault, (2) the vertical extent of the slip zone associated with these creep events is greater than about 0.5 km but perhaps not more than a couple of kilometers, (3) nonseismic episodic slip on this part of the San Andreas fault does not appear to propagate uniformly over more than a couple of kilometers, and (4) the model presented in this paper requires 0.5–1.0 mm of dip-slip displacement to reproduce the residual deflection in the creep-related tilt wave forms observed.

INTRODUCTION

Prior to the installation of the U.S. Geological Survey tilt meter network, changes in the local tilt field were monitored with isolated instruments [*Sassa and Nishimura*, 1956; *Caloi*, 1958; *Hagiwara and Rikitake*, 1967; *Ostrovskii*, 1972; *Wood and Allen*, 1971]. *Wideman and Major* [1967] and *Berg and Lutschak* [1973] reported strain steps of 10^{-10}–10^{-6} after earthquakes that ranged in magnitude from 3.0 to 8.5. Theoretical predictions of the far field tilt response have shown that for elastic and anelastic dislocation models, residual tilt fields as large as 10^{-9}–10^{-8} rad are to be expected at distances of several thousand kilometers from major earthquakes [*Chinnery*, 1961; *Press*, 1965; *Rosenman and Singh*, 1973]. Although quasi-static analyses have been used [e.g., *Press*, 1965; *Ben-Menahem et al.*, 1969], it is expected that nonseismic slip will alter the tilt field in the same fashion as seismic slip.

Fault creep has been monitored instrumentally at multiple sites along the San Andreas fault since 1968 [*Yamashita and Burford*, 1973; *Nason et al.*, 1974]. Episodic slip of 1–10 mm with durations of a few hours is quite common along the San Andreas fault in central California [*King et al.*, 1973; *Nason*, 1973], particularly at the Melendy Ranch (MEL) site, where creep events with a 4- to 6-month recurrence interval have been observed [*Nason*, 1973].

Changes in the local strain field that were similar in form to creep events have been reported by *Stewart et al.* [1973] and *Bufe and Tocher* [1974] for a strain meter at the Stone Canyon Geophysical Observatory south of Hollister, California. The March 15, 1972, strain event had a maximum strain change of approximately 10^{-6}. This event was interpreted as creep related, although the strain change in time at points not on the fault would not necessarily be expected to have the same form as the displacement on the fault. No solution utilizing pure right lateral strike-slip motion of constant magnitude was found to be satisfactory. The more general solution incorporating time varying strike-slip and dip-slip displacement on a laterally and vertically propagating slip zone could reproduce the observed strain event. One feature of the solution was that the dip-slip component equaled the strike-slip component in magnitude about 15 minutes after the start of the event, although it decayed rapidly thereafter, as would be expected if a mixed dislocation formed the slip zone boundary.

In this paper, short-period (i.e., minutes to tens of hours) tilt fluctuations with residual displacements (hereafter called SR events) observed at four central California sites are examined to determine what changes in the local tilt field as a function of time and distance from the fault might be expected when episodic nonseismic slip occurs on the San Andreas fault, and a model compatible with the creep-related tilt events at MEL [*Johnston et al.*, 1976] is presented.

INSTRUMENTATION

There are approximately 18 tilt meters in operation along the San Andreas fault in central California; five have been recording data since 1973. In addition, a network of approximately 30 creep meters has operated in the same area during the same time period. Figure 1 shows the locations of the tilt meters and creep meters used in this investigation and their relation to the San Andreas fault. The interstation distances and station-to-fault distances are recorded in Table 1. A description of tilt meter installation, operation, and preliminary results is contained in the work by *Johnston and Mortensen* [1974] and *Mortensen and Johnston* [1975] and of creep meter in the work by *Yamashita and Burford* [1973] and *Nason et al.* [1974].

RESULTS AND DISCUSSION

The data from four tilt meters (SAS, LIB, MEL, BVY) and several creep meters (XPR1, XFL1, and the array at MEL; see Figure 1) were examined to search for correspondence in signals and hence to determine the wave form amplitude and duration of possible creep-related tilt fluctuations. The group of SR events was selected because of their similarity to the duration and slip amplitude change of creep event displacements on the San Andreas fault. It is not likely that these events are due to instrumental or site installation effects because the event duration is generally much longer than the instrumental time constants and because tilt events were ob-

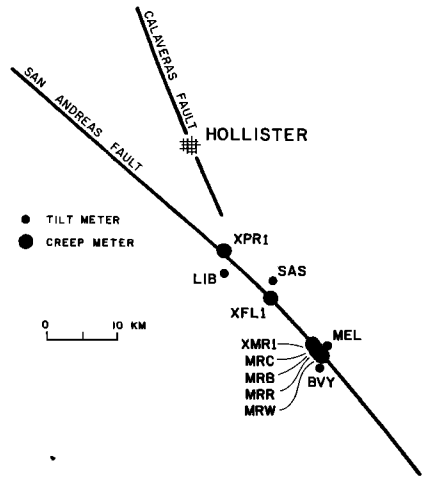

Fig. 1. Location of instruments used in this investigation.

TABLE 1. Interstation and Station-to-Fault Distances

	Distance, km
LIB-XPR1	3.4
LIB-SAS	7.0
XPR1-XFL1	9.2
SAS-XFL1	2.0
BVY-XMR1	2.4
BVY-MEL	2.2
MEL-XMR1	0.84
XFL1-XMR1	11.2
SAS-fault	1.3
LIB-fault	2.0
MEL-fault	0.37
BVY-fault	1.6

Instrument locations: LIB, 36°41.67'N, 121°20.60'W; SAS, 36°41.00'N, 121°16.08'W; MEL, 36°35.38'N, 121°10.63'W; BVY, 36°34.27'N, 121°11.23'W; XFL1, 36°39.9'N, 121°16.3'W; XPR1, 36°43.4'N, 121°20.9'W; XMR1, 36°35.7'N, 121°11.2'W.

served simultaneously at SAS and 20 m from SAS on a second tilt meter (SAN) before SAN was removed for repair.

The category of SR events encompasses amplitude changes of 0.01–1.5 μrad with durations of minutes to tens of hours. A catalog of the SR event occurrence times was compiled from the original records for each tilt meter. To relate episodic nonseismic slip on the San Andreas fault to specific short-period perturbations in the local tilt field, the tilt event catalog was compared to a list of the occurrence times of earthquakes at distances less than 10 source dimensions from the tilt meters and to the local rainfall record. Those SR events that appeared to be caused by local earthquakes and rainfall are the subject of another study and are not considered here.

Although specific rainfall-related changes in tilt amplitude could be removed in this fashion, the broader question of a possible seasonal pattern to the occurrence of SR events is less clear. A histogram of event frequency versus time (Figure 2) appears to show a seasonal variation in the number of events at LIB with more events in June, July, and August than in other months. The pattern at the other stations is not as well defined, although MEL recorded slightly fewer events during the dry season. Seasonal fluctuations in tilt event frequency may indicate changes in pore fluid pressure related to rainfall-induced changes in water level [*Nur and Booker*, 1972].

To examine in more detail the character of the short-period wave forms, some of the events from each station remaining in the catalog were enlarged from the original record, digitized, and computer processed to a uniform scale. Examples of these events are shown in Figures 3, 5, 6, and 7. The detailed nature of the wave shapes shows great variability, but the general features can be grouped into steplike, impulsive, and antisymmetric wave forms, more complex forms consisting of combinations of these groups.

If these features are a response to propagating nonseismic episodic slip over many tens of kilometers of the San Andreas fault, then a space-time plot of the short-period events should show some coherence that can be related to the growth of the slip zone. Figure 4 shows the occurrence times of the SR events excluding rainfall and coseismic events for the tilt meters and creep meters shown in Figure 1. The dashed lines indicate a period of no data, and the different symbols indicate the amplitude of the events. Because the tilt meters in principle are affected by slip at depth, any buried slip should appear as a tilt perturbation. Consequently, any large-scale pattern of slip that produces residual tilt displacements should appear in this catalog whether or not the slip zone intersects the ground surface (i.e., appears as a surface creep event). The lack of coherence between events on different tilt meters then may be interpreted as indicating that either (1) the SR events are not due to nonseismic episodic slip on the San Andreas fault, (2) nonseismic slip occurring on the San Andreas fault does not generally result in residual tilt displacements above a level of 10^{-8} rad for most sites 1–3 km from the fault, or (3) nonseismic slip occuring on the San Andreas fault does not propagate coherently over distances comparable to the instrument spacing (i.e., about 5–10 km).

To investigate these possibilities, portions of the raw tilt records within ±24 hours of creep events observed on nearby creep meters were checked. For the three instrument groups in this study, only one (the MEL array) showed any consistent pattern of amplitude changes associated with creep events [*Johnston et al.*, 1976]. (A creep-related tilt event has also been observed at the Cienega Winery south of Hollister, California [*Mortensen et al.*, 1975].)

The null results of comparing creep event to tilt event occurrence times at XFL1-SAS and XPRI-LIB suggest that creep events of 3 mm or less will probably not be seen on tilt meters with a sensitivity of 10^{-8} rad located more than 0.5–1.0 km from the fault either because (1) the slip zone associated with the creep event is quite restricted spatially or because (2) the strain field is concentrated closer to the fault, owing perhaps to low rigidity within the fault zone. A very large slip zone or slip magnitude on the fault could produce the amplitudes and wave forms observed at LIB and SAS, but lack of coherency of these events suggests that the length of the slip zone is less than the instrument spacing. Amplification of the signal due to a source on the fault is unlikely because the creep events at XFL1 and XPR1 are not observed at SAS and LIB, respectively. But if (1) the slip zone dimension is less than the instrument spacing, (2) the slip magnitude is of the same order as the creep events, and (3) no signal amplification occurs, then the predicated amplitudes at SAS and LIB will be much less than those observed. This and the possible seasonal variation in tilt event frequency suggest that nonseismic SR events observed at distances of more than 1 km from the fault (i.e., LIB, SAS, BVY) and most if not all of those events not specifically related to creep (e.g., at MEL) may be due to some local strain release mechanism near the instrument rather than

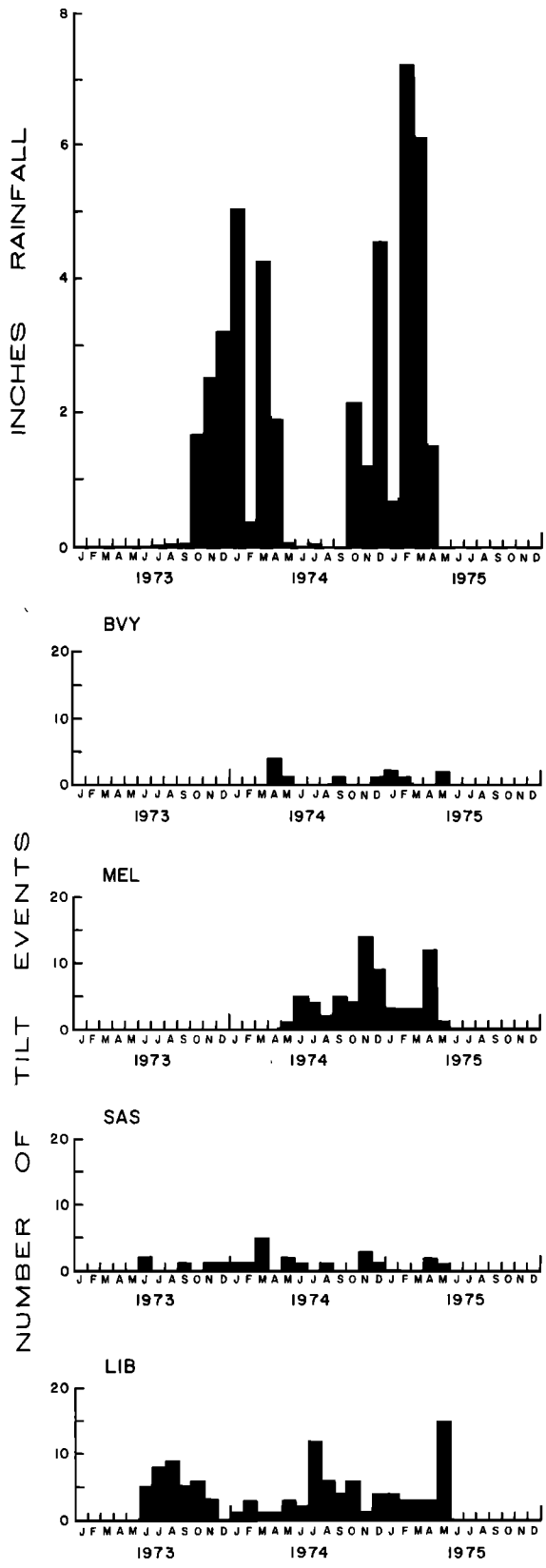

Fig. 2. Nonseismic SR event frequency at the stations listed and local rainfall data from June 1973 to April 1975. Tilt data end in May 1975. Start-up of tilt meters is indicated by the first nonzero data block.

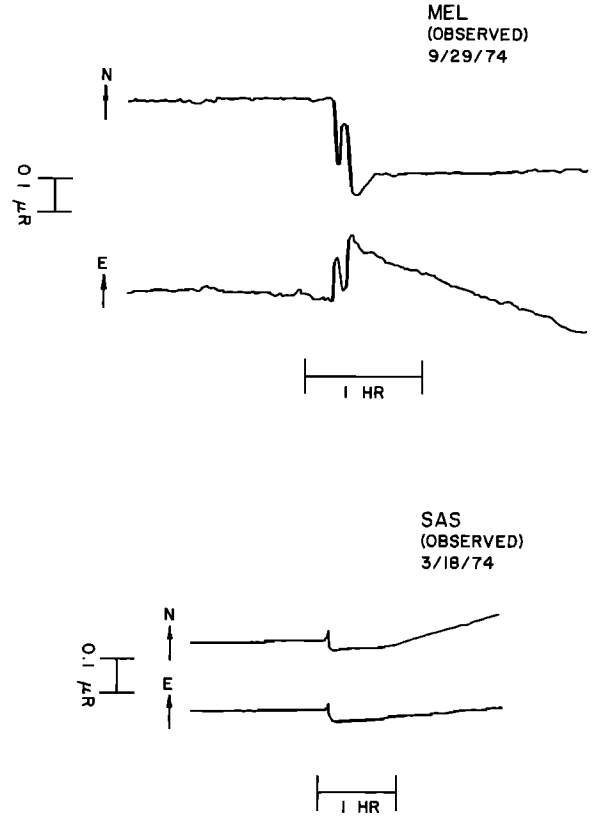

Fig. 3. Examples of the variation in wave forms of nonseismic short-period tilt perturbations with residual deflections.

a source on the fault, although the possibility of contamination from instrumental or site installation effects cannot be totally disregarded.

The creep-related tilt events at MEL and the lack of coherency between tilt events on different tilt meters and between the SAS-XFL1 and LIB-XPR1 groups suggested that more specific information about the physical details of propagating episodic slip on the local tilt field was required. A quasi-static model of the slip process was constructed by using the analytic expressions for tilt on the free surface due to a vertical rectangular dislocation surface embedded in an elastic half space [*Press*, 1965]. The slip zone coordinates and the amount of slip were incremented to simulate the growth of the slip zone. The effect of the slip magnitude change in time, the area of the zone, the growth of the zone relative to the station, and the type of slip on the tilt wave form, symmetry, and residual displacement was determined by using this model. The observed residual displacements could be produced by changes in strike-slip or dip-slip amplitude in time, by propagating dip-slip displacement of constant magnitude, or by a zone boundary near the instrument. The model wave forms were compared to the observed events, and by trial and error the specific slip zone geometries were determined for some of the events. Two examples are shown in Figure 5; the observed event is shown in the left column, the best-fit model wave form produced by using strike-slip motion in the middle, and the strike-slip zone geometry on the right. The solutions for these observations are not unique, although eventually multiple observations of the same event will constrain the possible models when an inversion technique is used to determine which geometry provides the closest match to the observed wave form. Bounds could then be placed on the parameters of interest [*Stewart et*

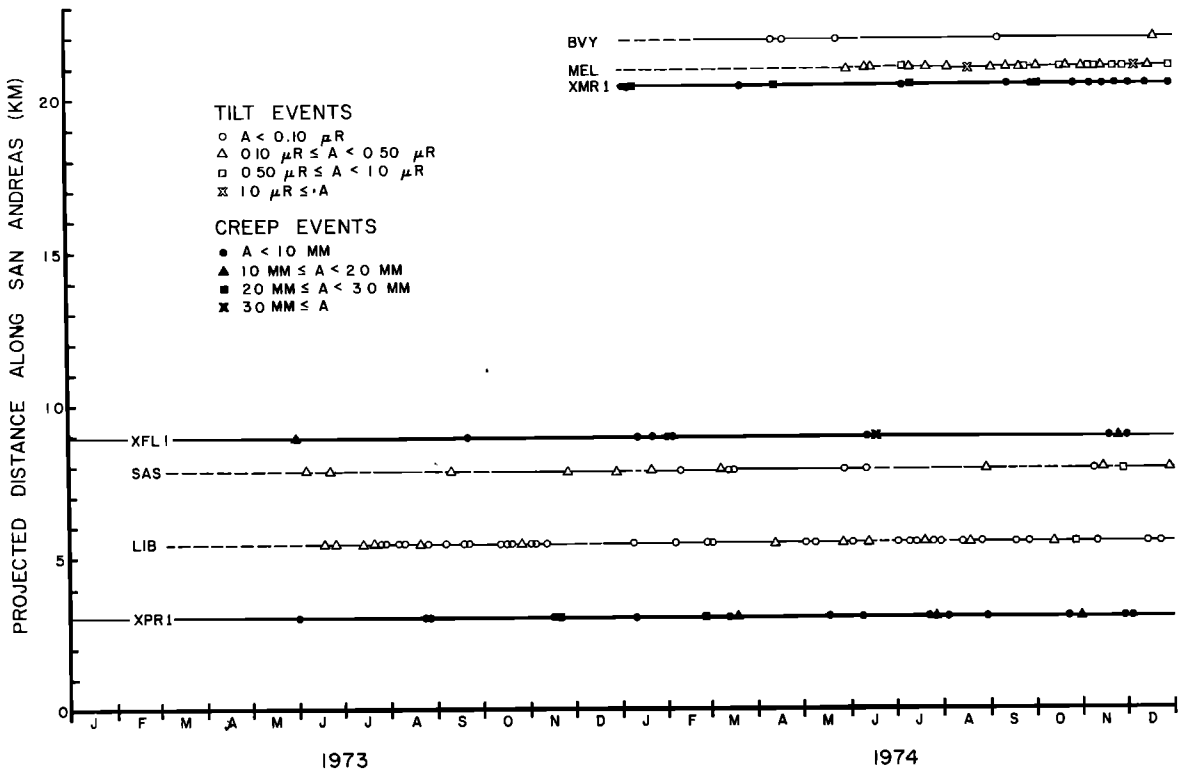

Fig. 4. Space-time distribution of creep events and nonseismic SR events. The magnitude of the residual deflection (i.e., amplitude of the difference vector) is indicated by the different symbols.

al., 1973]. The LIB event, for example, can also be reproduced by using dip-slip displacement increasing in time on a stationary zone, whereas the SAS event can be reproduced by using dip-slip displacement propagating from NW to SE. One major result of comparing the predicted to observed amplitudes is that 3–10 mm of pure strike-slip displacement on the San Andreas fault will not yield the observed change in tilt amplitude and thus suggests that local strike-slip or dip-slip motion on subsidiary fractures is responsible for many of the observed events. This model does demonstrate that the SR event wave forms are compatible with a few specific slip zone configurations and puts constraints on the direction of propa-

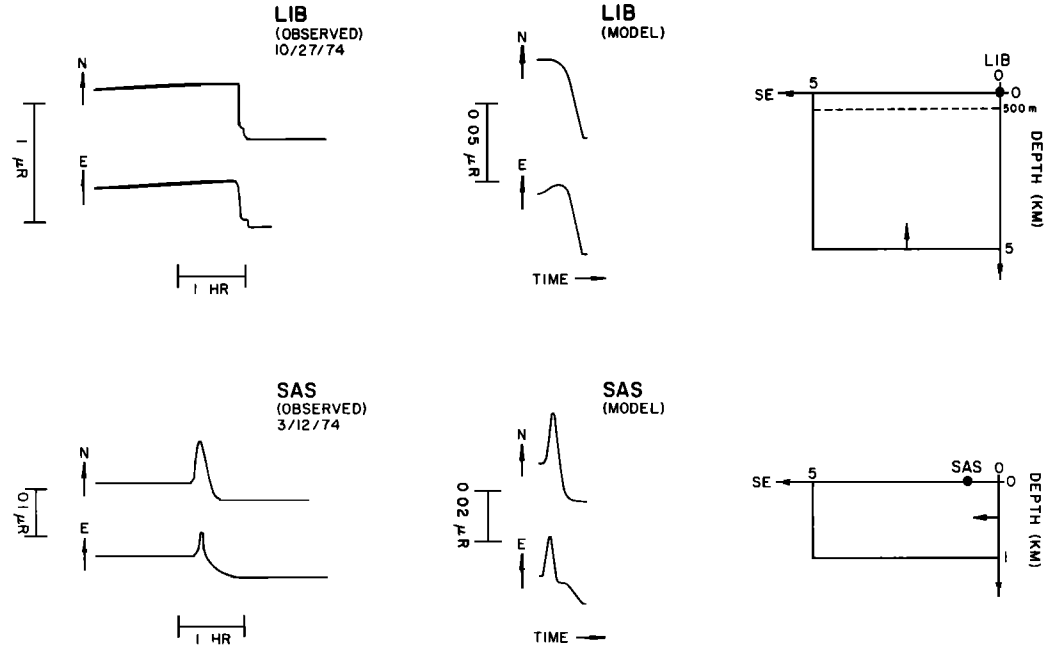

Fig. 5. Two nonseismic SR events. The wave forms in the middle column are the closest match to the observed wave shapes using the quasi-static dislocation model (see text) and pure strike-slip displacement for a propagating slip zone (as shown in the right-hand column) on the San Andreas fault. The slip zone expands in the direction and from the boundary indicated by the arrow.

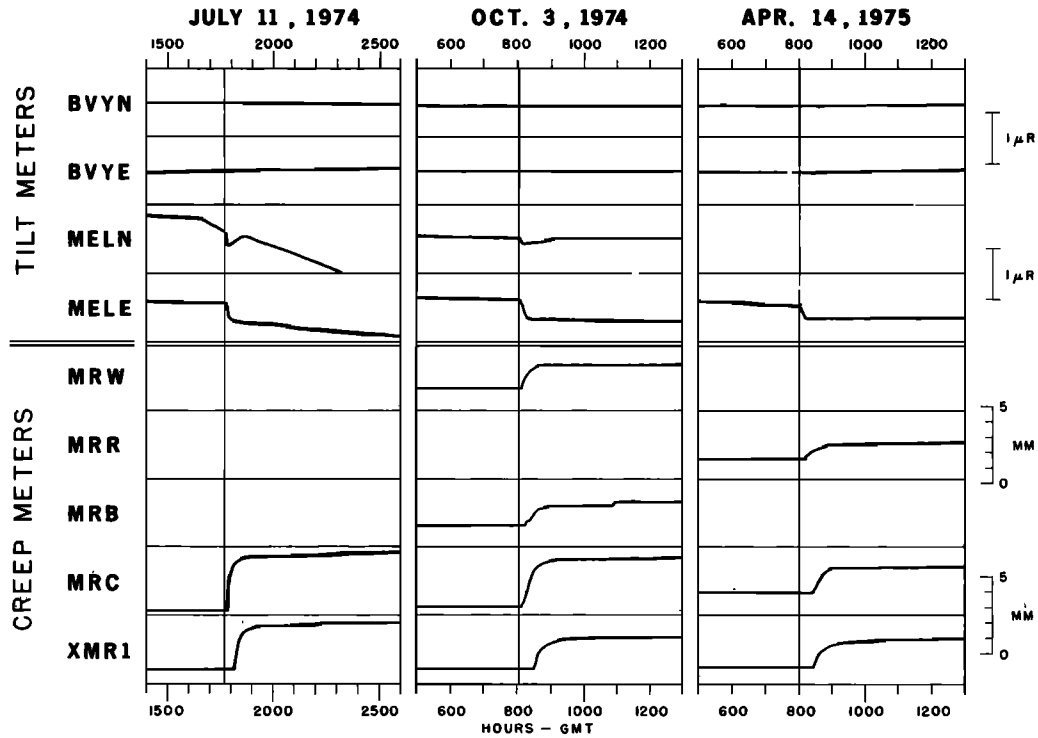

Fig. 6. The creep-related tilt events observed at MEL and the associated creep records. No signal above 10^{-8} rad was recorded by BVY. (Deflections down to the north (N) and east (E) are positive.) The linear southward deflection on MELN (July 11, 1974, event) may be due to local ground noise. [From *Johnston et al.*, 1976.]

gation and type of slip that can be associated with any given perturbation.

The model was also used to reproduce the tilt and creep events seen at MEL, a station much closer to the fault than the others. These data, summarized by *Johnston et al.* [1976], are reproduced in Figure 6. The most important features of these records are (1) the initial SW deflection at MEL, (2) the residual westward displacement, (3) an apparent propagation from SE to NW suggested by the creep event onset times, and (4) the lack of observable signal above 10^{-8}-rad resolution at BVY.

A set of possible slip zone configurations was determined for

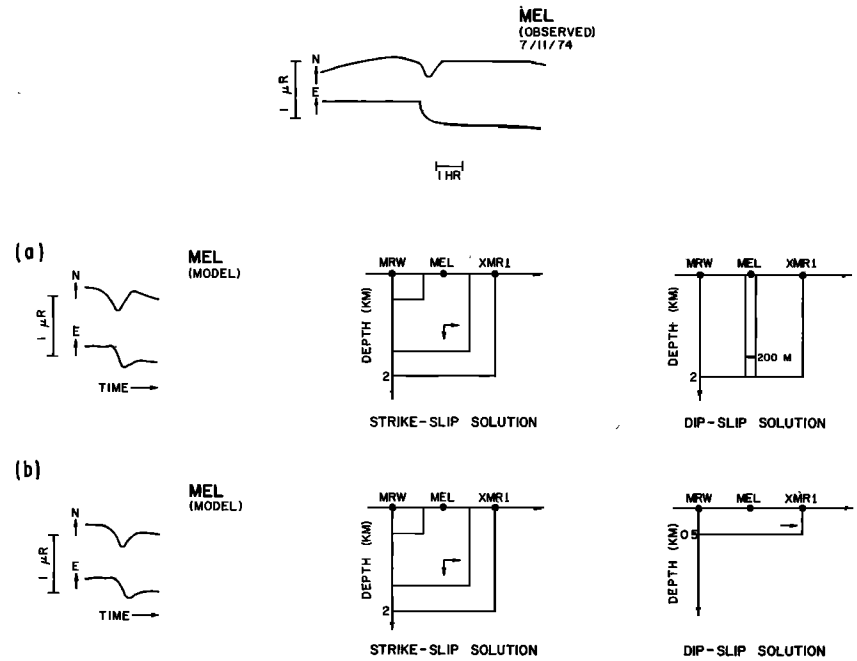

Fig. 7. Two models of propagating slip that reproduce the initial SW deflection and residual westward displacement for creep-related tilt events at MEL. In both cases the strike-slip zone expands SE to NW and down from MRW. The dip-slip also expands SE to NW but in one case is confined to ±100 m about MEL and in the other is confined to the upper 500 m. The strike-slip displacement increased from 0 to 3 mm right lateral, the dip-slip from 0 to 1.0 mm (*a*) or 0.5 mm (*b*), MEL side down; the slip was incremented from its initial to final value in a $(1 - e^{-t/\tau})$ fashion. The projection of MEL onto the fault is indicated by the dot. The slip zone expands in the direction and from the boundary indicated by the arrow.

this data set by trial and error by using the quasi-static model. It was determined that no solution utilizing 3–10 mm of pure strike-slip displacement was compatible with both the creep and tilt data sets. However, when a small amount of dip-slip displacement (i.e., 0.5–1.0 mm with the northeast side down) was added to the solution, the predicted wave forms and amplitudes closely matched those observed. Two possible slip zone configurations that reproduce the important features of the tilt wave form at MEL are shown in Figure 7. In both cases the strike-slip zone propagates laterally and vertically (SE to NW and down, starting at or south of MRW), with right lateral slip incremented from 0 to 3 mm in a $(1 - e^{-t/\tau})$ fashion. The dip-slip solutions correspond to lateral SE to NW propagation, but in Figure 7*a* the dip-slip is confined to a region ±100 m about the projection of MEL onto the fault and extends 2 km in depth (a configuration perhaps indicated by a small fault scarp near MEL [*Johnston et al.*, 1976]), while in Figure 7*b* it is confined to the upper 500 m (but travels from MRW to XMR1). The dip-slip magnitude in Figure 7*a* is 1.0 mm and in Figure 7*b* is 0.5 mm, both incremented from zero to their final value in a $(1 - e^{-t/\tau})$ fashion, northeast side down. Both models produce a slight eastward recovery, but increasing the amount of dip-slip or decreasing the strike-slip somewhat reduces the amount of the recovery.

The lower boundaries of the slip zones are somewhat arbitrary since the near-field wave form and amplitude are insensitive to the exact depth. Because MEL is 370 m from the fault the slip zone depth must be $\gtrsim$0.5 km. However, if bounds can be placed on the dip-slip magnitude and zone configuration, then bounds can be placed on the strike-slip solution because the resultant wave form is a compromise between these two solutions.

The slip zone configurations and slip magnitudes shown in Figure 7 were used to predict the tilt change at BVY. The maximum tilt amplitude predicted at BVY is 0.02 μrad; although this is near the present instrument resolution (10^{-8} rad), it should have been observable. If the model is realistic, the lack of signal at BVY may indicate a change in material properties between the fault and BVY.

Conclusions

The short-period tilt data suggest that (1) a change in tilt amplitude of 10^{-8}–10^{-6} rad associated with creep events will be observed only if the tilt meter is less than 0.5–1.0 km from the fault trace, (2) the vertical extent of the slip zone associated with surface creep events may be less than a couple of kilometers but greater than about 0.5 km, (3) creep events on this part of the San Andreas fault do not appear to propagate uniformly over more than a couple of kilometers, and (4) the model presented in this paper suggests that about 0.5–1.0 mm of dip-slip displacement is required to produce the residual deflection in the tilt wave forms observed at MEL during a creep event [*Johnston et al.*, 1976].

References

Ben-Menahem, A., S. J. Singh, and F. Solomon, Static deformation of a spherical earth model by internal dislocations, *Bull. Seismol. Soc. Amer., 59,* 813–853, 1969.

Berg, E., and W. Lutschak, Crustal tilt fields and propagation velocities associated with earthquakes, *Geophys. J. Roy. Astron. Soc., 35,* 5–29, 1973.

Bufe, C. G., and D. Tocher, Central San Andreas fault: Strain episodes, fault creep, and earthquakes, *Geology, 2,* 205–207, 1974.

Caloi, P., About some phenomena preceding and following the seismic movements in the zone characterized by high seismicity, *Contrib. Geophys., 1,* 44–56, 1958.

Chinnery, M. A., The deformation of the ground around surface faults, *Bull. Seismol. Soc. Amer., 51,* 355–372, 1961.

Hagiwara, T., and T. Rikitake, Japanese program on earthquake prediction, *Science, 157,* 761–768, 1967.

Johnston, M. J. S., and C. E. Mortensen, Tilt precursors before earthquakes on the San Andreas fault, California, *Science, 186,* 1031–1034, 1974.

Johnston, M. J. S., S. McHugh, and R. O. Burford, On simultaneous tilt and creep observations on the San Andreas fault, *Nature, 260,* 691–693, 1976.

King, C. Y., R. D. Nason, and D. Tocher, Kinematics of fault creep, *Phil. Trans. Roy. Soc. London, Ser. A, 274,* 355–360, 1973.

Mortensen, C. E., and M. J. S. Johnston, The nature of surface tilt along 85 km of the San Andreas fault—Preliminary results from a 14-instrument array, *Pure Appl. Geophys., 113,* 237–249, 1975.

Mortensen, C. E., R. C. Lee, and R. O. Burford, Simultaneous tilt, strain, creep, and water level observations at the Cienega Winery south of Hollister, California (abstract), *Eos Trans. AGU, 56,* 1059, 1975.

Nason, R. D., Time regularity of fault creep events, Earthquake Research in NOAA, 1971-1972, *Tech. Rep. ERL 256-ESL 28,* pp. 24–26, Nat. Oceanogr. and Atmos. Admin., Boulder, Colo., 1973.

Nason, R. D., F. R. Philippsborn, and P. A. Yamashita, Catalog of creepmeter measurements in central California from 1968 to 1972, *Open File Rep. 74-31,* U.S. Geol. Surv., Washington, D. C., 1974.

Nur, A., and J. R. Booker, Aftershocks caused by pore fluid flow?, *Science, 175,* 885–887, 1972.

Ostrovskii, A. Y., On variations in tilts of the earth's surface before strong near earthquakes, in *Physical Bases of Seeking Methods of Predicting Earthquakes,* translated from Russian by D. B. Vitaliano, pp. 58–61, Academy of Sciences of the USSR, Moscow, 1972.

Press, F., Displacements, strains, and tilts at teleseismic distances, *J. Geophys. Res., 70,* 2395–2412, 1965.

Rosenman, M., and S. J. Singh, Quasi-static strains and tilts due to faulting in a viscoelastic half-space, *Bull. Seismol. Soc. Amer., 63,* 1737–1752, 1973.

Sassa, K., and E. Nishimura, On phenomena forerunning earthquakes, *Bull. Disaster Prev. Res. Inst. Kyoto Univ., 13,* 1, 1956.

Stewart, R. M., C. G. Bufe, and J. H. Pfluke, Creep-caused strain events at Stone Canyon, California, Proc. Tectonic Problems of the San Andreas fault, *Stanford Univ. Publ. Univ. Ser. Geol. Sci., 13,* 286–293, 1973.

Wideman, C. J., and M. W. Major, Strain steps associated with earthquakes, *Bull. Seismol. Soc. Amer., 57,* 1429–1444, 1967.

Wood, M. D., and R. V. Allen, Anomalous microtilt preceding a local earthquake, *Bull. Seismol. Soc. Amer., 61,* 1801–1809, 1971.

Yamashita, P. A., and R. O. Burford, Catalog of preliminary results from an 18-station creepmeter network along the San Andreas fault system in central California for the time interval June 1969 to June 1973, open file report, U.S. Geol. Surv., Washington, D. C., 1973.

(Received June 1, 1976;
revised August 11, 1976;
accepted August 11, 1976.)